

Conductivity behavior & reduction of TiO₂NTs filled with NiFe₂O₄ quantum dots

A. A. Farghali^{1,*}, M. Bahgat², A. F. Moustafa¹

¹Nano Science and Nanotechnology Unit, Chemistry Department, Faculty of Science, Beni-Suef University, Egypt

²Central Metallurgical Research and Development Institute (CMRDI), Minerals Technology Department, Pyrometallurgy laboratory, Helwan, Egypt

d_farghali@yahoo.com

Abstract: TiO₂ nanotubes anatase phase (TiO₂NTs) were prepared by hydrothermal approaches followed by ion exchange and phase transformation process. The obtained TiO₂NTs were then filled with NiFe₂O₄ quantum dots (Q.Ds) under vacuum. The obtained nanomaterials were used to study the influence of the filling process on the conductivity behavior in a hydrogen flow (1 L/min) at different temperatures (500-700°C). It was found that the electric conductivity increased by increasing the gas exposure time and the reduction temperature that illustrates the semiconductor behavior of the nanomaterials. Empty anatase phase TiO₂NTs achieved the highest values of conductivity at 550 and 600°C, but at higher temperatures (650 and 700°C) the conductivity decreases by increasing temperature due to the destruction of tubular form. The conductivity mechanism of TiO₂NTs towards H₂ gas was discussed. Further investigation for the reduction behavior by thermogravimetric technique was carried out. The activation energy values were calculated to determine the rate controlling mechanism.

[A.A. Farghali, M. Bahgat, A. F. Moustafa. **Conductivity behavior & reduction of TiO₂NTs filled with NiFe₂O₄ quantum dots.** *J Am Sci* 2013;9(4):77-86].(ISSN: 1545-1003). <http://www.jofamericanscience.org>. 11

Key Words: Reduction kinetics, electrical conductivity, anatase TiO₂NTs, filled TiO₂NTs and Quantum dots.

1. Introduction

One-dimensional nanostructured TiO₂ are of great interest for possible applications such as high effect solar cell (Bach *et al.*, 1998), photocatalysts (Yu *et al.*, 2003), gas sensor (Taurino *et al.*, 2003), molecular straws (Pederson and Broughton, 1992) and semiconductor devices. This wide range of applications is due to their nanotubular structure, high specific surface area, ion-changeable ability and size-dependent properties. Currently developed methods of fabricating TiO₂-based nanotubes comprise the assisted-template method (Lee *et al.*, 2005), the sol-gel process (Liu *et al.*, 2008), electrochemical anodic oxidation (Tsuchiya *et al.*, 2005), and hydrothermal treatment (Thorne *et al.*, 2005). The hydrothermal process is suitable for large scale production, able to yield very low dimensional, well separated, crystallized nanotubes and a pure-phase structure (Ou and Lo, 2007). On the other hand the synthesis and characterization of TiO₂NTs or modified TiO₂NTs are generally studied (Ghicov *et al.*, 2006; Macak *et al.*, 2007). It was reported that site-selective deposition of Pt nanoparticles on a titania nanotube (TNT) was investigated in order to improve the photocatalytic activity of a TNT (Nishijima *et al.*, 2008). Also CdS and S⁶⁺-modified TiO₂ nanotubes were prepared to enhance the visible light activity of TiO₂ (Zhang *et al.*, 2009). Recently, various studies showed that doping TiO₂ nanotubes with different quantum dots (CdS, CdTe, PbS, CdSe, InAs etc.) could significantly enhance their visible light response through narrowing the band gap, and

hence shift their absorbance to the visible region (Yu *et al.*, 2006; HongMei *et al.*, 2008; Ratanatawanate *et al.*, 2008; Gao *et al.*, 2009; Cheng *et al.*, 2011). The thermal stability of TiO₂NTs was one of the essential criteria of their reaction with gases, where titania has earned much attention for its oxygen sensing capabilities (Rothschild *et al.*, 2000). Furthermore with proper manipulation of the microstructure, crystalline phase and/or addition of proper impurities or surface functionalization titania can also be used as a reducing gas sensor (Savage *et al.*, 2002). The interaction of a gas with a metal oxide semiconductor is primarily a surface phenomenon, therefore nanoporous metal oxides (Koch, 2003) offer the advantage of providing large sensing surface areas. The conductivity behavior of TiO₂ in reducing atmosphere is still controversial. The conductivity in TiO₂ nanocrystal depends on defects within the crystal lattice and the oxygen vacancies (Millot *et al.*, 1987). The defects may be point defect "oxygen vacancies or Ti interstitials", or two dimensional planer defects known as crystallographic shear planes (CSP) (Sorensen, 1981). The reduction process leads to very small loss of oxygen from rutile. This assumption is substantiated by experimental evidence since TiO₂ does not undergo much weight loss upon reduction and the value of x in TiO_(2-x) can be extremely small (x ≤ 0.001). This leads to the formation of oxygen vacancies which act as active sites in which hydrogen quickly adsorbed. The two electrons of the oxygen vacancies are transferred to the conduction band of TiO₂ enhancing its

conductivity (Khader *et al.*, 1993). It was reported that in steady state conditions at 713-788K, the specific catalytic activity of hydrogen oxidation on rutile is one order of magnitude higher than that of anatase due to the different bond strength of the surface oxygen (Shimanovskaya *et al.*, 1983). Not only the TiO₂ phase type but also, loosening of oxygen and hence oxygen vacancies formation control the conductivity behavior of TiO₂. These factors depend mainly on; reaction temperature, nature of reducing gas, the extent of reduction and the defects density (Khader *et al.*, 1993). The conductivity mechanism of anatase phase TiO₂NTs towards H₂ gas was discussed by several researchers (Birkefeld *et al.*, 1992; Varghese *et al.*, 2003). It was reported that the increase in conductivity is not due to the hydrogen removing oxygen from the lattice or the removing of chemisorbed oxygen but because the nanotubes are conductor in oxygen atmosphere (Varghese *et al.*, 2003). Other investigators suggested diffusion mechanism, but it is not the dominant mechanism behind high conductivity of TiO₂ nanotubes (Birkefeld *et al.*, 1992). On the other hand conduction in ferrites is a combination of electronic and ionic that is significantly affected by the oxygen vacancies and/or lattice defects within the sample. Generally, the oxygen absorption/desorption into/from the sample affects the oxygen stoichiometry and hence the conductivity (Patrakeevea *et al.*, 2005). In fact, thermal treatment of ferrites in a reducing gas environment modifies the material morphology as well as introducing metallic atoms into the ferrite crystals thus; an increase in the saturation magnetization was achieved (Ebrahimi *et al.*, 1999). In the present investigation the three catalysts "NiFe₂O₄, empty anatase phase TiO₂NTs and anatase phase TiO₂NTs filled with NiFe₂O₄ Q.Ds" were used to study the influence of the filling process on the conductivity behavior in a hydrogen gas flow (1 L/min) at different temperatures (500-700°C).

2. Experimental

Anatase phase TiO₂ NTs were prepared via hydrothermal treatment at 150°C for 144 hrs flowed by ion exchange reaction and thermal treatment at 500°C for 2hrs. The filling process of the anatase TiO₂NTs with NiFe₂O₄ Q.Ds was carried out under vacuum. In this novel method a mixed solution of Ni-Fe nitrates with a molar ratio of 1:2 was allowed to enter the titanium oxides NTs under vacuum, then stirring occurred for about 30 min. using a magnetic stirrer. The mixture was then kept overnight, filtered and washed with distilled water. The precipitate was added to a beaker containing 50 mL of 1 M NaOH and stirred for 30 min. at 60°C, filtered, washed well with distilled water, then dried at 100°C for 1 hr and

finally fired at 600°C for 3 hrs. The filling percentage was calculated from semi quantitative analysis (S.Q) obtained from XRD patterns to be 18.8%.

NiFe₂O₄ were prepared by self flash combustion method from nitrates precursors (Farghali *et al.*, 2008). The three catalysts were moistened with few drops of distilled water. Equal weights were pressed into cylindrical compacts with 1cm diameter and 0.5 cm thickness, followed by drying process at 85°C for 1 h. The electrical conductivity for all samples was measured to obtain the influence of the filling process on the conductivity behavior during hydrogen gas flow. The reduction assembly and gas flow system used in this study were previously mentioned (Farghali *et al.*, 2008). The electrical conductivity cell was made of two ceramic circular bases joined together by four stainless steel rods as shown in figure 1. For conductivity dynamics during hydrogen gas flow, the sample compact was placed between the two stainless steel electrodes and held tightly with the springs, the compacts were left at the operating temperature (500 - 700°C) for about 30 min in nitrogen gas atmosphere, and then, hydrogen gas is passed (1 L/min). The total resistance, R, of samples was measured directly using a computerized Avometer. The data is transferred into electrical conductivity (σ) using the equation ($\sigma = l / (R.A)$), where l is the length and A is the cross-section area.

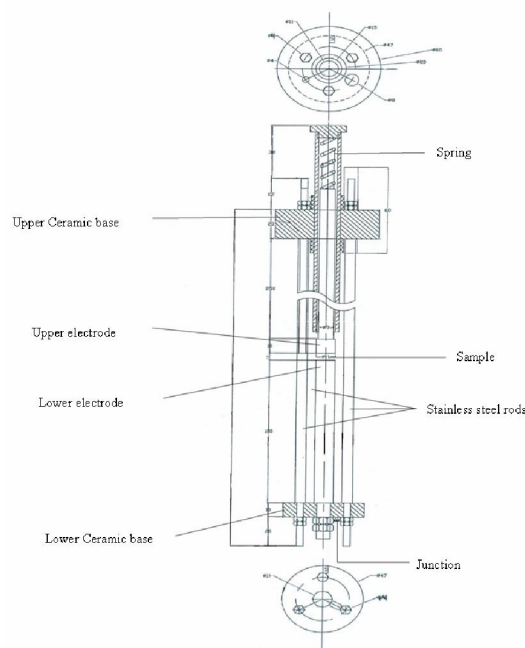


Figure (1); Schematic diagram of the conductivity cell

The reduction kinetics was further investigated using thermogravimetric measurements. In this experiment, the oxygen weight loss during hydrogen reduction is measured directly by a digital balance. The reduction kinetics is studied by measuring the reduction percentage as a function of time during hydrogen gas flow. The obtained results were compared with that obtained by in situ conductivity measurements.

The phase identification and crystal size of the obtained nanomaterials before and after reduction were deduced by XRD analysis (JSX-60P JEOL diffractometer). The average crystal size was calculated using the XRD peaks with the application of a software computer programme TOPAZ2 depending on the following Scherer's formula

$$D = \frac{0.9 \lambda}{\beta \cos \theta}$$

where D is the crystallite size, λ the X-ray wave length, β the broadening of the diffraction peak and θ is the diffraction angle. The influence of the reduction process on the surface morphology and particles size of the nanomaterials were deduced using TEM (JEOL JEM-1230 TEM). The absorption spectra of empty TiO₂NTs and that filled with NiFe₂O₄ was measured using UV-visible (UV-vis) spectrometer (Jasco V-350).

3. Results and Discussion.

3.1. Physicochemical characterization of the materials.

Figure 2 illustrates the XRD patterns of NiFe₂O₄ prepared by self flash combustion method of nitrate precursors, anatase phase TiO₂NTs and anatase phase TiO₂NTs filled with NiFe₂O₄ quantum dots. It can be deduced that pure phase of NiFe₂O₄ with crystallite size ranging from 9 to 16nm was obtained. The X-ray Diffractogram of the anatase phase TiO₂NTs filled with NiFe₂O₄ quantum dots reveals that a certain interaction occurs between the two phases as a result of the filling process which was more confirmed by measuring the UV absorbance of the empty and filled TiO₂NTs (Figure 3). The microstructure of the prepared NiFe₂O₄ was investigated by TEM (Figure 4). It can be seen that NiFe₂O₄ almost has round shape with particle size ranging from 9 to 12 nm which confirms the obtained data from XRD. Figure 5a illustrates TEM images of empty anatase phase TiO₂NTs revealing a tubular structure with varying lengths (ranging from 50 to 200 nm) and diameters (ranging from 3 to 10 nm). Figure 5b illustrates TEM images of the filled anatase phase TiO₂NTs revealing a homogeneous filling with the NiFe₂O₄ quantum dots.

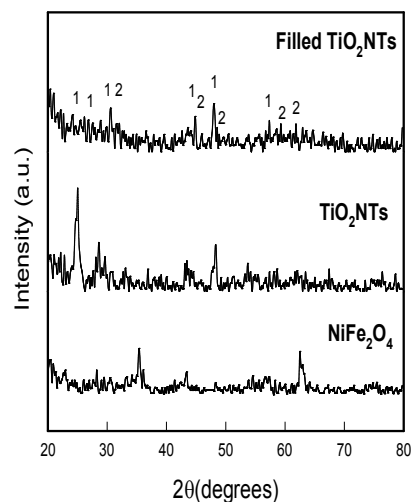


Figure 2: XRD patterns of NiFe₂O₄, empty anatase phase TiO₂NTs and TiO₂NTs filled with NiFe₂O₄ Q.Ds where (1) TiO₂NTs and (2) NiFe₂O₄

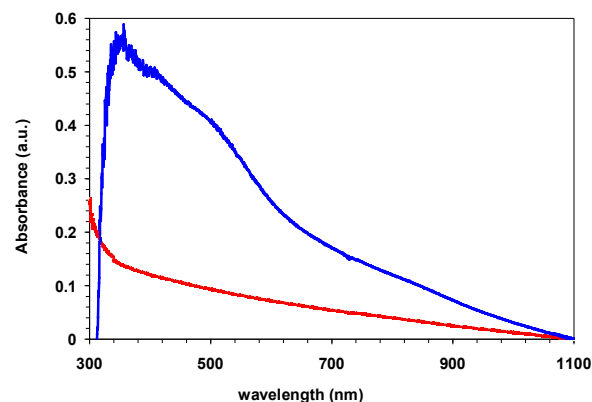


Figure 3; UV-vis absorption spectra for (a) anatase phase TiO₂NTs filled with NiFe₂O₄ Q.Ds and (b) empty anatase phase TiO₂NTs.

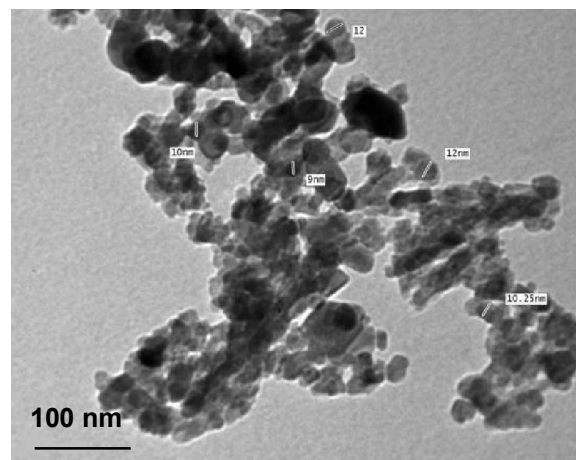


Figure 4: TEM image of NiFe₂O₄ prepared by self flash combustion method

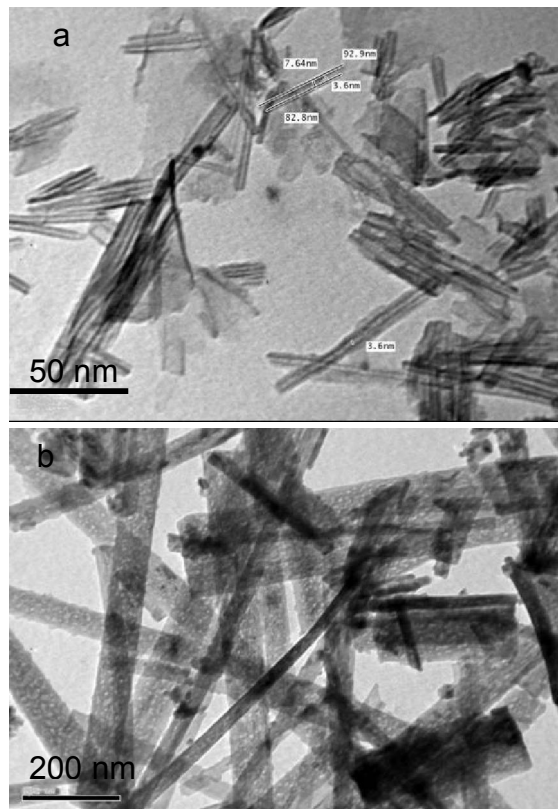


Figure 5; TEM images of:
 (a) empty anatase phase TiO_2NTs
 (b) anatase phase TiO_2NTs filled with NiFe_2O_4 Q.Ds

3.2. Conductivity of NiFe_2O_4

Figure 6 shows the variation of the electric conductivity of NiFe_2O_4 nanocrystals with time in a hydrogen flow (1 L/min) at different temperatures (500 -700°C). Generally, it is observed that the electric conductivity increased by increasing the temperature, which confirms that NiFe_2O_4 is an n-type semiconductor and electrons are the major carriers. During hydrogen exposure, oxygen from the surface as well as from the bulk is removed as water molecules and conducting electrons are lifted behind without molecular orbital to accommodate them. These free electrons are transferred into the conduction band resulting in decreasing the sample resistance and increasing its electronic conductivity. Figure 7 illustrates the XRD of NiFe_2O_4 before and after reduction at different temperatures (500 to 700°C). It was observed that Ni-Fe nano-alloy was formed at all reduction temperatures which can be attributed to the low preparation temperature of NiFe_2O_4 (600°C) (Farghali *et al.*, 2008). The oxides which are formed in formation of Ni-Fe nano-alloy may increase the ionic conductivity as well as the electronic conductivity and hence the total conductivity is increased. A complete reduction is

recognized by minimum resistant readings, while conductivity change with time is an indication of reduction rate. The reduction process is terminated as the conductivity change with time becomes minimal. It is clear that the time required for complete reduction decreased by increasing reduction temperature from 500 up to 700°C. The temporal changes of conductivity found to be significantly affected by the operating temperature (Farghali, *et al.*, 2008). The total conductivity is increased to a maximum value at 650°C (Curie temperature). The conductivity values at lower temperatures (500, 550, 600°C) are lower than that observed at 650°C. So the conductivity change rate is a function of the reduction rate and hence is determined by the chemistry of gas solid interaction, which is thermally activated by the operating temperature.

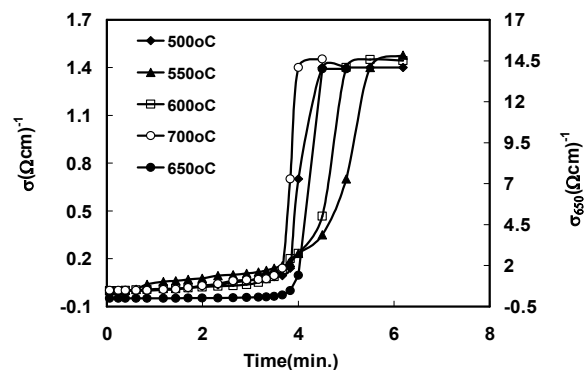


Figure 6: Conductivity transients of NiFe_2O_4 at various temperatures (500-700°C) during hydrogen gas flow of 1L min⁻¹ at constant pressure.

3.2 Conductivity of empty anatase phase TiO_2NTs

Figure 8 represent the variation of electrical conductivity, $\sigma(\Omega\text{cm})^{-1}$, of empty anatase TiO_2 nanotubes with reduction time during hydrogen gas flow (1 L/min) at various temperatures (500 to 700°C) and constant pressure. From figure (8) it can be deduce that empty TiO_2 nanotubes have variable conductivity behavior in reducing atmosphere at various temperatures i.e. this behavior is temperature dependent. The conductivity values increase by increasing reduction temperature and give their maximum values at 550, and 600°C ($\sigma \sim \infty$). At higher temperature (650 and 700°C) the conductivity decreases which may be attributed to destruction of the tubular form and their transformation to nanorods then nanoparticles (Zhang *et al.*, 2007). This behavior illustrates the role of tubular form in the conductivity of TiO_2 NTs. Figure 9 shows the XRD patterns of the anatase phase TiO_2NTs reduced at different temperatures (500 to 700°C). It can be obtained that the reduction of the anatase phase TiO_2 NTs leads to

transformation to rutile and other phase of TiO_2 , where this transformation is temperature dependent. In steady state conditions at 713-788K the specific catalytic activity of hydrogen oxidation on rutile is one order of magnitude higher than that of anatase due to the difference bond strength of the surface oxygen (Shimanovskaya *et al.*, 1983).

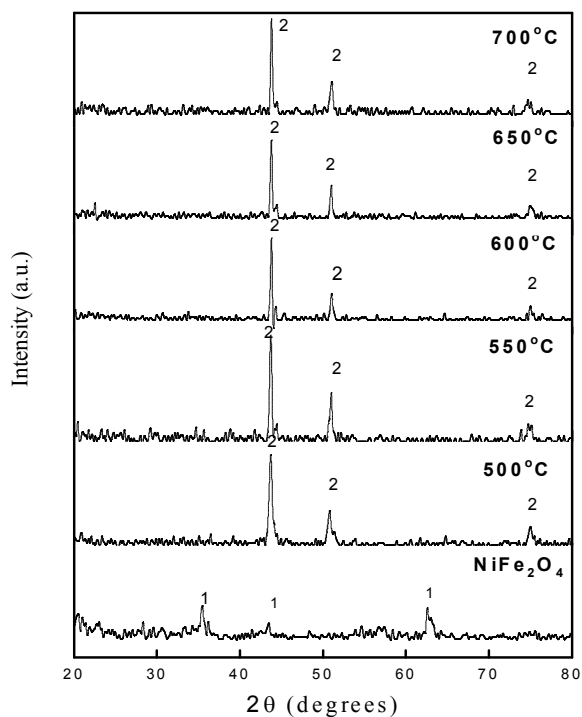


Figure 7: XRD diffractograms of unreduced NiFe_2O_4 nanocrystals compact and nanocrystals completely reduced at different temperatures (500-700°C) (1) NiFe_2O_4 and (2) Ni-Fe alloy.

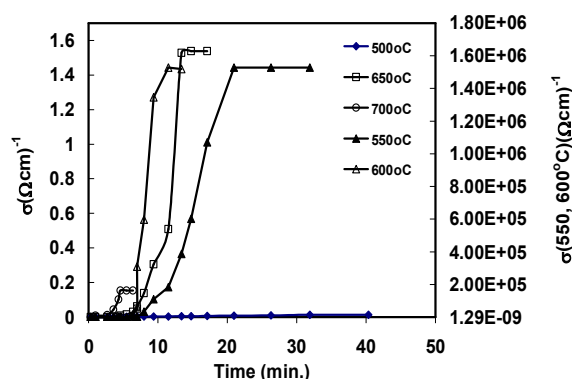


Figure 8; Variation of electrical conductivity, $\sigma(\Omega\text{cm})^{-1}$, of empty anatase phase TiO_2 nanotubes with time of reduction during hydrogen gas flow (1 L/min) at various temperatures (500 – 700°C) and constant pressure

The bond energy of the surface oxygen on anatase (243kJ/mol) is much higher than on rutile (159kJ/mol). On the other hand by using the anatase phase TiO_2 in nano-tubular form a new remarkable behavior and values in conductivity were observed. At reduction temperature 550°C, the formed phases are anatase and rutile as deduced from figure 9. These nanotubes phases achieved infinite conductivity ($\sigma = \infty$) i.e. the nanotubes becomes superconductors at these conditions as illustrated from figure 6. At reduction temperature 600°C, the nanotubes phases achieve infinite conductivity also, ($\sigma = \infty$), but in presence of anatase phase and TiO_2 with no evidences for presence of rutile phase as elucidated from figure 9. Thus, the infinite value of conductivity doesn't depend on the presence of rutile phase i.e. the hydrogen oxidation on the surface of anatase phase in tubular form is higher than that in bulk form. This may be attributed to the high specific surface area and size dependent properties which lead to an increase in defects density and oxygen vacancies, and hence an increase in the conductivity.

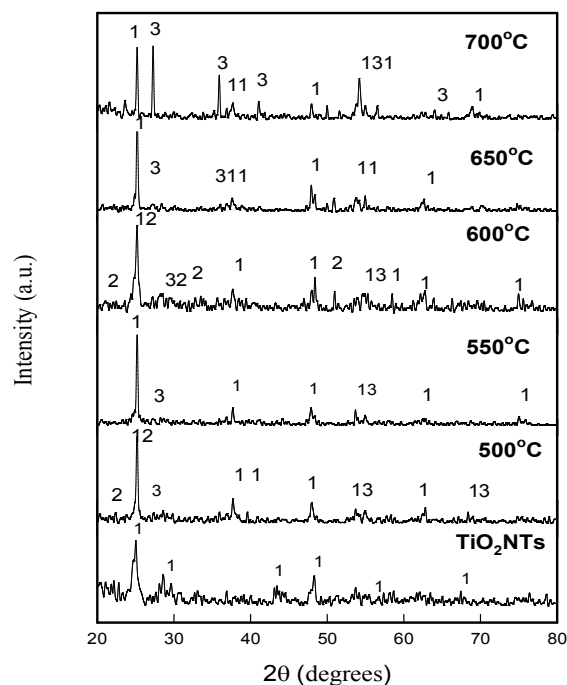


Figure 9; XRD diffractograms of anatase TiO_2NTs reduced at different temperatures (500-700°C). (1) anatase TiO_2 , (2) TiO_2 oxide, and (3) rutile TiO_2

Conductivity mechanism of anatase phase TiO_2 NTs towards H_2 gas

There are many suggested mechanisms for this unusual enhancement of TiO_2 nanotubes conduction in presence of hydrogen gas. One of them is the diffusion mechanism (Birkefeld *et al.*, 1992) and the second is the splitting hydrogen atoms mechanism

over Pt electrode (Raupp and Dumesic, 1985). In the present investigation the observed behavior has great agreement with the dominated mechanism "chemisorptions of the splitting hydrogen atoms" (Varghese *et al.*, 2003). In this mechanism, Pt electrode played important role in hydrogen splitting and the charges transfer from the adsorbed layer to the nanotubes but, in the present experiments the nanotubes achieved infinite conductivity without using Pt electrodes.

3.3 Conductivity of anatase phase TiO₂NTs filled with NiFe₂O₄ Q.Ds

Figure 10 represents the variation of electrical conductivity, σ (Ωcm)⁻¹, with reduction time for anatase phase TiO₂ nanotubes filled with NiFe₂O₄ Q.Ds in hydrogen gas flow (1 L/min) at various temperatures (500 – 700°C) and constant pressure. The conductivity of filled nanotubes increases with increasing reduction temperature, which confirms that filled TiO₂NTs are n-type semiconductors and electrons are the major carriers. Figure 10 also shows a regular increase of conductivity, but with lower values than that observed with empty anatase phase TiO₂ NTs. In this case, the conductivity depends not only on adsorption of hydrogen on defects within the crystal lattice but also on the reduction of NiFe₂O₄ Q.Ds. Every removed oxygen atom leave behind two electrons without orbital to accommodate. These electrons are transferred to conduction band of TiO₂NTs, and increasing their conductivity. So, the Fermi level of TiO₂NTs equilibrates fast with energy level of surface adsorbate hydrogen layer. Accordingly the hydrogen desorption in atomic form takes place by transferring an electron back to the adsorbate (Varghese *et al.*, 2003), or may be the semiconductor Q.Ds "NiFe₂O₄" and/or their reduction products act as center for electrons and holes recombination. This will lead to decreasing in the conductivity value.

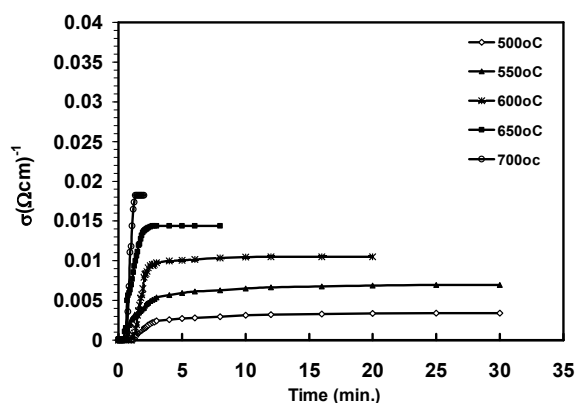


Figure (10); variation of electrical conductivity, σ (Ωcm)⁻¹, with time of reduction for filled anatase TiO₂ nanotubes with NiFe₂O₄ Q.Ds during hydrogen gas flow (1 L/min) at various temperatures (500 – 700°C) and constant pressure

Figure 11 represents the XRD patterns of TiO₂NTs filled with NiFe₂O₄ Q.Ds before and after reduction at different temperature. It can be observed that by increasing the reaction temperature the reduction percentage increased producing different oxides and Ni-Fe alloy depending on the operating temperature. Formation of different oxide phases and transformation of these oxides from valance state to another may increases the ionic conductivity as well as the electronic conductivity and hence the total conductivity is increased. The conductivity values for empty and filled NTs reduced at various temperatures (500-700°C) are illustrated in Table1. The highest value of conductivity was observed for the filled NTs almost near the lowest value for the empty NTs.

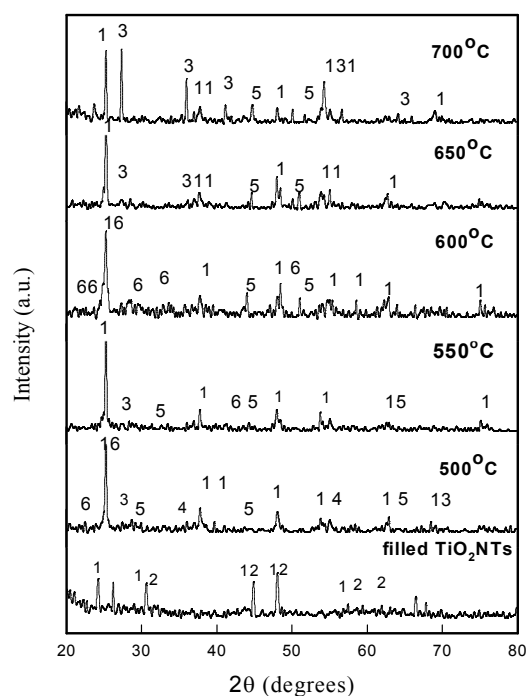


Figure (11); XRD diffractograms of TiO₂NTs filled with NiFe₂O₄ Q.Ds reduced at various temperatures (500-700°C) (1) TiO₂NTs anatase (2) NiFe₂O₄ (3) Rutile, (4)Fe₂O₃ (5)Ni-Fe alloy and (6) TiO₂ oxide.

3.4 Reduction kinetics

Further investigation of nanocrystalline NiFe₂O₄ reduction kinetics was studied by thermogravimetric technique, in which the reduction kinetics was studied by calculating the reduction percentage as a function of the hydrogen gas exposure time. A set of dynamic curves similar in methodology to those obtained by dynamic conductivity measurements are obtained. Figure 12 shows the reduction percentage at various temperatures (500-700°C) of NiFe₂O₄ compacts in constant hydrogen gas flow of 1 L min⁻¹ and constant

pressure. It is clear that NiFe_2O_4 continue to lose its oxygen content gradually during hydrogen exposure. These results are in consistence with that obtained from dynamic conductivity and XRD. In the reduction of empty anatase phase TiO_2NTs the measurements can not be carried out due to the small portion of removed oxygen to be detected by the electrical balance as illustrated above. On the other hand the thermogravimetric measurements were done for the anatase phase TiO_2NTs filled with NiFe_2O_4 Q.Ds.

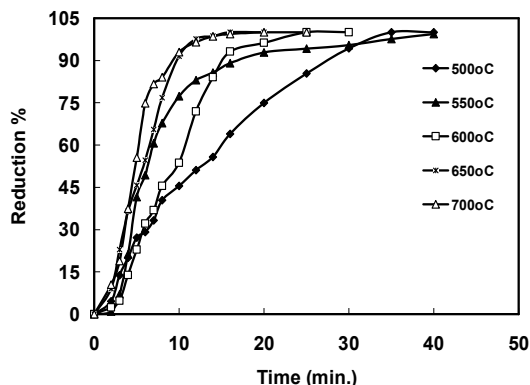


Figure 12: Reduction percentage at various temperatures (500-700°C) of NiFe_2O_4 nanocrystal compacts during a constant hydrogen gas flow of (1 L min^{-1}) and at constant pressure.

Figure 13 illustrates the reduction percentage of TiO_2 NTs filled with NiFe_2O_4 Q.Ds. It was obtained that by increasing temperature from 500 to 700°C the reduction percentage increased. The reduction achieves the highest values at higher temperatures (600 - 700°C) corresponding to complete reduction of NiFe_2O_4 Q.Ds and formation of Ni-Fe nanoalloy. At lower reduction temperatures (550, 550°C) the filled TiO_2NTs achieved uncompleted reduction compared with free NiFe_2O_4 . This may be attributed to lower gas diffusion at lower reduction temperatures between NiFe_2O_4 and TiO_2NTs , while at higher temperatures there is enough activation energy for Hydrogen gas diffusion needed for complete reduction. TEM analysis for the samples reduced at higher temperatures (600 - 700°C) reflected the optimum conditions required for formation of Ni-Fe Q.Ds with keeping the tubular texture of TiO_2NTs . Figures 14 (a, b, c, d, e) represent TEM images of anatase phase TiO_2NTs filled with NiFe_2O_4 Q.Ds reduced at 600, 650 and 700°C respectively during hydrogen gas flow. It can be deduced that reduction at 600°C almost preserves the tubular structure of TiO_2NTs (figure14a), while reduction at 650°C the tubular texture of the NTs starts to deform and

aggregate as illustrate in figure 14 (b, c). The deformation and breakdown increased at higher temperature (700°C) where as the nanotubes changed to nanorods then nanoparticles as appear from figure 14(d, e).

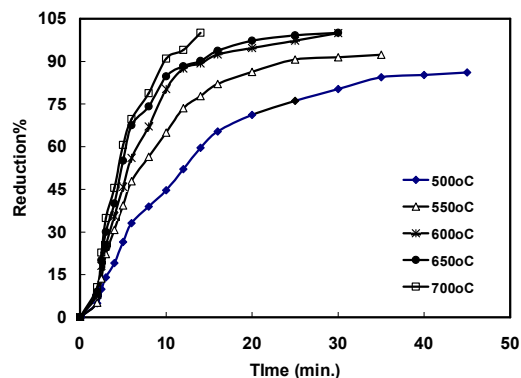
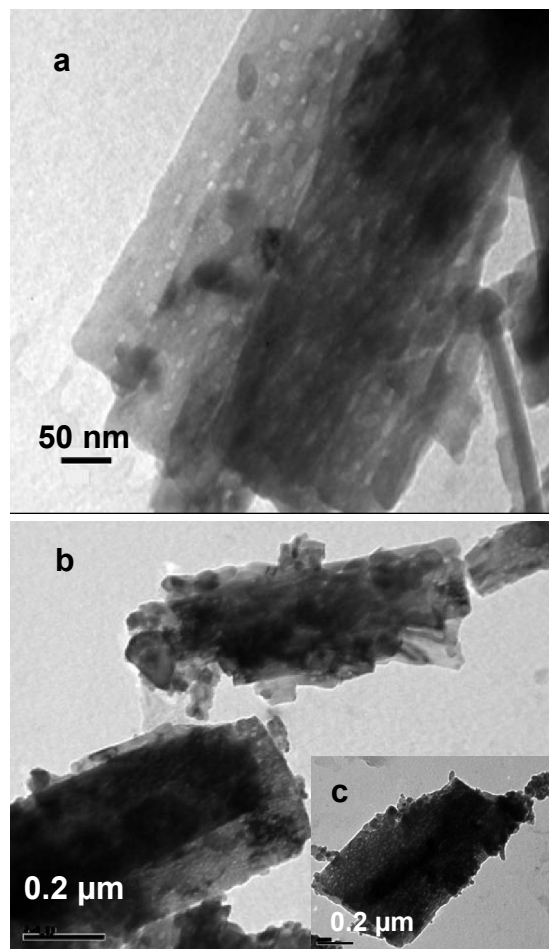


Figure 13; General reduction behavior at various temperatures for TiO_2NTs compacts filled with NiFe_2O_4 QDs in hydrogen gas flow of (1 L min^{-1}) at constant pressure.



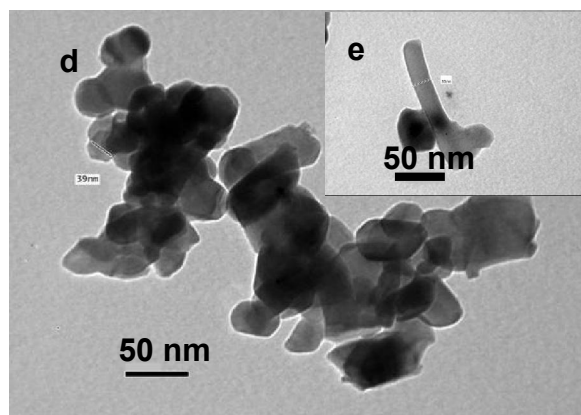


Figure 14; TEM images of filled TiO₂NTs reduced at (a) 600°C, (b, c) 650°C and (d, e) 700°C in hydrogen gas flow (1 L/min) and constant pressure

3.5 Activation Energy Ea

The general ranges of activation energy values have been calculated by many investigators in order to determine the rate controlling mechanism (Strangway, 1964). These values were recently proved by other studies (El-Geassy *et al.*, 2004). Utilizing Arrhenius relation and plotting the rate constant as a function of the reduction temperature, the activation energy can be calculated. Figure 15 (a, b, c, d, e,) give such straight line relationship deduced from the conductivity and thermogravimetric curves for NiFe₂O₄, empty anatase phase TiO₂NTs, and anatase phase TiO₂NTs filled with NiFe₂O₄ Q.Ds respectively. For NiFe₂O₄ the overall Ea values obtained from conductivity and thermogravimetric measurements are greatly closed to each other "42.75 and 43.2kJ/mol respectively ". This confirms that reaction controlling mechanism is combined gas diffusion and interfacial chemical (Strangway, 1964). For empty anatase phase TiO₂NTs the overall activation energy value deduced from conductivity measurements is calculated to be 45.6kJ/mol, which indicates that the rate controlling mechanism is the combined gas diffusion and interfacial chemical reaction. Also the activation energy value indicates that the adsorption of hydrogen on the empty anatase phase TiO₂NTs surface is considered to be chemisorption which confirms the conductivity mechanism "chemisorptions of the splitting hydrogen atoms". On the other hand the activation energy values for anatase phase TiO₂NTs filled with NiFe₂O₄ Q.Ds were calculated to be 37.3 and 33 kJ/mol which indicate that the rate controlling mechanism is the combined mechanism gas diffusion and interfacial chemical reaction. The value of activation energy obtained from conductivity technique is approximately closes to that obtained from thermogravimetric technique. The value of

activation energy for the empty TiO₂NTs was higher than that for filled TiO₂NTs which can be attributed to the filling process of TiO₂NTs with NiFe₂O₄ Q.Ds. Figure 3 represents the UV-vis absorption spectra of empty anatase phase TiO₂NTs and anatase phase TiO₂NTs filled with NiFe₂O₄ Q.Ds. The NiFe₂O₄ Q.Ds narrow the band gap of TiO₂NTs and shift their absorption edge to the visible region. The threshold edges of the empty anatase phase TiO₂NTs and filled TiO₂NTs are 396 and 770 nm respectively. The band gap absorption edge of the samples was determined according to the relation (Wang *et al.*, 2006; Zhang *et al.*, 2009)

$$E_g = \frac{1240}{\lambda}$$

where λ is the optical absorption threshold. The estimated band gaps are 3.13 and 1.61 eV which reflect the difference in Ea values for the empty anatase phase TiO₂NTs and anatase phase TiO₂NTs filled with NiFe₂O₄ Q.Ds respectively.

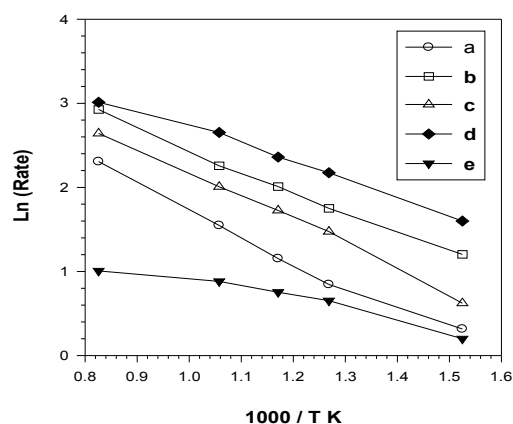


Figure 15; Arrhenius plots of reduction of NiFe₂O₄ as deduced from (a) conductivity measurement (b) thermogravimetric measurements.(c) empty anatase phase TiO₂NTs as deduced from conductivity measurements, and anatase phase TiO₂NTs filled with NiFe₂O₄ Q.Ds as deduced from (d) conductivity measurements and (e) thermogravimetric measurements

Table 1; The conductivity values of empty and filled TiO₂NTs reduced at various temperatures (500-700°C)

Temperature °C	$\sigma(\Omega\text{cm})^{-1}$ empty NTs	$\sigma(\Omega\text{cm})^{-1}$ filled NTs
500	0.014	0.0034
550	∞	0.007
600	∞	0.011
650	1.54	0.014
700	0.153	0.018

4. Conclusion

Anatase phase TiO₂ nanotubes prepared by hydrothermal method followed by thermal treatment at 500°C for 2hrs were successfully filled with NiFe₂O₄ Q.Ds. The conductivity behavior of empty anatase TiO₂NTs, the filled anatase TiO₂NTs and NiFe₂O₄ Q.Ds was studied in a hydrogen gas flow (1 L/min) at different temperatures (500-700°C). The electric conductivity of the three nanomaterials increased by increasing the reduction temperature, which illustrates the semiconductor behavior of the three nanomaterials.

Empty anatase phase TiO₂NTs achieved the highest values of conductivity at 550 and 600°C. But at higher temperature (650, 700°C) the conductivity decreases by increasing temperature which may be attributed to the destruction of tubular form of nanotubes. The mechanism of conductivity of anatase phase TiO₂ nanotubes towards H₂ gas was found to be chemisorption of splitting hydrogen atoms mechanism.

Depending on conductivity and thermogravimetry techniques the activation energy values were calculated to determine the rate controlling mechanism. The all catalysts have the same mechanism "combined gas diffusion and interfacial chemical reaction mechanism. NiFe₂O₄ Q.Ds narrow the band gap of TiO₂NTs and shift their absorption edge to the visible region.

Acknowledgment

"The present research is supported by The Science and Technology Development Fund (STDF), Egypt

Corresponding author:

Dr. Ahmed Ali Farghali

Chemistry Department, Faculty of Science, Beni-Suef University, Beni-Suef, 621111, Egypt.

E-mail: d_farghali@yahoo.com

References

- [1] Bach U., D. Lupo, P. Comte, J.E. Moser, F. Welssortels, J. Scallbeck, H. Spreitzer, M. Gratzel, "Solid-state dye-sensitized mesoporous TiO₂ solar cells with high photon-to-electron conversion efficiencies" *Nature* 395, (1998), 583-585.
- [2] Yu J.G., H.G. Yu, B. Cheng, X.J. Zhao, J.C. Yu, W.K. Ho, "The Effect of Calcination Temperature on the Surface Microstructure and Photocatalytic Activity of TiO₂ Thin Films Prepared by Liquid Phase Deposition" *J. Phys. Chem. B* 107, (2003), 13871-13879.
- [3] Taurino A.M., M. Epifani, T. Toccoli, S. Iannotta, P. Siciliano, "Innovative aspects in thin film technologies for nanostructured materials in gas sensor devices" *Thin Solid Films* 436, (2003), 52-63.
- [4] Pederson M.R., J.Q. Broughton, "Nanocapillarity in fullerene tubules" *Phys. Rev. Lett.* 69, (1992), 2689-2692.
- [5] Lee J.H., I.C. Leu, M.C. Hsu, Y.W. Chung, M.H. Hon, "Fabrication of aligned TiO₂ one-dimensional nanostructured arrays using a one-step templating solution approach" *J. Phys. Chem. B* 109, (2005), 13056-13059.
- [6] Liu L., T. Ning, Y. Rena, Z. Suna, F. Wang, W. Zhoua, S. Xie, L. Songa, S. Luoa, D. Li, J. Shen, W. Ma, Y. Zhoua, "Synthesis, characterization, photoluminescence and ferroelectric properties of PbTiO₃ nanotube arrays" *J. Mater. Sci. Engin. B* 149, (2008), 41-46
- [7] Tsuchiya H., J.M. Macak, L. Taveira, E. Balaur, A. Ghicov, K. Sirotna, P. Schmuki, "TiO₂ Nanotube Arrays: Synthesis, Properties, and Applications" *Electrochem. Commun.* 7 (2005) 576-580.
- [8] Thorne A., A. Kruth, D. Tunstall, J.T.S. Irvine, W. Zhou, "Formation, Structure, and Stability of Titanate Nanotubes and Their Proton Conductivity" *J. Phys. Chem. B* 109, (2005), 5439-5444.
- [9] Ou H. H., S.L. Lo, "Review of titania nanotubes synthesized via the hydrothermal treatment: Fabrication, modification, and application" *Separation and Purification Technology* 58, (2007), 179-191
- [10] Macak J.M., M. Zlamal, J. Krysa, P. Schmuki, "Self-Organized TiO₂ Nanotube Layers as Highly Efficient Photocatalysts" *Small* 3, (2007), 300-304.
- [11] Ghicov A., J.M. Macak, H. Tsuchiya, J. Kunze, V. Haeublein, L. Frey, P. Schmuki, "Ion Implantation and Annealing for an Efficient N-Doping of TiO₂ Nanotubes" *Nano. Lett.* 6, (2006), 1080-1082.
- [12] Nishijima K., T. Fukahori, N. Murakami, T. Kamai, T. Tsubota, T. Ohno, "Development of a titania nanotube (TNT) loaded site-selectively with Pt nanoparticles and their photocatalytic activities" *Appl. Catal. A: General* 337 (2008) 105-109.
- [13] Zhang X., L. Lei, J. Zhang, Q. Chen, J. Bao, B. Fang, "A novel CdS/S-TiO₂ nanotubes photocatalyst with high visible light activity" *Separation and Purification Technology* 66 (2009) 417-421
- [14] Cheng H., X. Zhao, X. Sui, Y. Xiong, J. Zhao, "Fabrication and characterization of CdS-sensitized TiO₂ nanotube photoelectrode" *Nanopart Res* 13, (2011), 555-562.

- [15] Gao X.-F., H.-B. Li, W.-T. Sun, Q. Chen, F.-Q. Tang, L.-M. Peng, "CdTe Quantum Dots-Sensitized TiO₂ Nanotube Array Photoelectrodes" *Phys. Chem. C* 113, (2009), 7531–7535
- [16] Ratanatawanate C., C. Xiong, K. J. Balkus, "Fabrication of PbS Quantum Dot Doped TiO₂ Nanotubes" *ACS nano*, 2, (2008), 1682-1688
- [17] HongMei Z., C. Ke, J. YanLing, L. XiaoLan, L. LinSong, Z. XingTang, D. ZuLiang, "Preparation of sodium titanate nanotubes modified by CdSe quantum dots and their photovoltaic characteristics" *Sci China Ser B-Chem.* 51, (2008), 976-982
- [18] Yu P., K. Zhu, A. G. Norman, S. Ferrere, A. J. Frank, A. J. Nozik, "Nanocrystalline TiO₂ Solar Cells Sensitized with InAs Quantum Dots" *Phys. Chem. B*, 110, (2006) 25451-25454
- [19] Rothschild A., F. Edelman, Y. Komem, F. Cosandey, "Sensing behavior of TiO₂ thin films exposed to air at low temperatures" *Sens. Actuators B* 67 (2000) 282.
- [20] Savage N., B. Chwiroth, A. Ginwalla, B.R. Patton, S.A. Akbar, P.K. Dutta, "Composite n-p semiconducting titanium oxides as gas sensors" *Sens. Actuators B* 79 (2002) 17-27.
- [21] Koch C.C., "Ductility in Nanostructured and Ultra Fine-Grained Materials: Recent Evidence for Optimism" *J. Metast. and Nanostructured Mater.*, 18, (2003), 9-20.
- [22] Millot F., M.-G. Blanchin, R. Tetot, J.-F. Marucco, B. Poumellec, C. Picard, B. Touzlin, "High temperature nonstoichiometric rutile TiO_{2-x}", *Prog. Solid State Chem.* 17, (1987), 263-293.
- [23] Sorensen, O. T., "Nonstoichiometric Oxides" Ed.; Academic Press: New York, 1981.
- [24] Khader M. M., F. M.-N. Kheiri, B. E. El-Anadouli, B. G. Ateya, "Mechanism of reduction of rutile with hydrogen" *J. Phys. Chem.* 97, (1993), 6074-6077
- [25] Shimanovskaya V. V., L.G. Svintsova, A.A. Dvernyakova, G.N. Novitskaya, G.I. Golodets, "Kinetics and mechanism of hydrogen oxidation on titanium dioxide (anatase and rutile)", *Rect. Kinet. Lett.*, 23, (1983), 37-41
- [26] Varghese O. K., D. Gong, M. Paulose, K. G. Ong, C. A. Grimes, "Hydrogen sensing using titania nanotubes" *J. Sens. and Actuat. B* 93 (2003) 338–344
- [27] Birkefeld L.D., A.M. Azad, S.A. Akbar, "Carbon Monoxide and Hydrogen Detection by Anatase Modification of Titanium Dioxide" *J. Am. Ceram. Soc.* 75, (1992), 2964-2968.
- [28] Patrakeeva M.V., I.A. Leonidova, V.L. Kozhevnikova, K.R. Poeppelmeier, "p-Type electron transport in La_{1-x}Sr_xFeO_{3-d} at high temperatures", *J. Solid State Chemistry* 178 (2005) 921–927
- [29] Ebrahimi S. A. S., C. B. Ponton, I. R. Harris, A. Kianvash, "Optimization of the coercivity-modifying hydrogenation and re-calcination processes for strontium hexaferrite powder synthesized conventionally", *J. of Mater. Scien.*, 34, (1999), 35-43
- [30] Farghali A.A., M. H. Khedr, A. F. Moustafa, "Photocatalytic activity and magnetic properties of nanocrystallite strontium hexaferrite prepared by self-flash combustion", *Mater. Techno.* 23, (2008), 104-109.
- [31] Khedr M. H., "Isothermal reduction kinetics at 900–1100 °C of NiFe₂O₄ sintered at 1000–1200 °C", *J. Anal. Appl. Pyrolysis*, 73 (2005) 123-129.
- [32] Fargali A. A., M. K. Zayed, M. H. Khedr and A. F. Moustafa, "Phase and conductivity dynamics of strontium hexaferrite nanocrystals in a hydrogen gas flow", *Interna. J.of Phys. Scien.* Vol. 3, (2008), 131-139.
- [33] Zhang L., H.Lin, N. Wang, C. Lin, J. Li, "The evolution of morphology and crystal form of titanate nanotubes under calcination and its mechanism", *J Allo. and Compo.* 431 (2007) 230–235
- [34] Raupp G.B., J.A. Dumesic, "Adsorption of carbon monoxide, carbon dioxide, hydrogen, and water on titania surfaces with different oxidation states", *J. Phys. Chem.* 89 (1985) 5240-5246.
- [35] Strangway P. K., M.Sc. Thesis, "Kinetics of Reduction of Iron Oxide by Reformed Natural Gas", Toronto University. (1964).
- [36] El-Geassy A. A., M. I. Nasr, M. H. Khedr, K. S. Abdel-Halim, "Reduction behaviour of iron ore fluxed pellets under load at 1023-1273 K", *ISIJ Int.* 44, (2004), 462-469.
- [37] Wang N., H. Lin, J. Li, X. Yang, B. Chi, C. Lin, "Effect of annealing temperature on phase transition and optical property of titanate nanotubes prepared by ion exchange approach", *Alloys and Comp.* 424 (2006) 311–314.